

Conversion of Methane over Bimetallic Copper and Nickel Actinide Oxides (Th, U) Using Nitrous Oxide As Oxidant

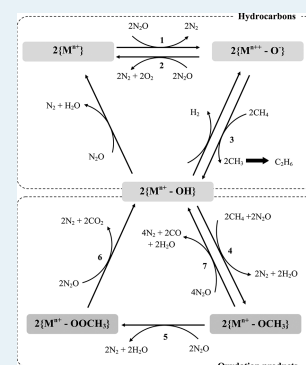
Joaquim B. Branco,^{*,†} Ana C. Ferreira,[†] Ana M. Botelho do Rego,[‡] Ana M. Ferraria,[‡] and Teresa Almeida-Gasche[†]

[†]Unidade de Ciências Químicas e Radiofarmacêuticas, IST/ITN—Campus Tecnológico e Nuclear, Instituto Superior Técnico, Universidade Técnica de Lisboa, Estrada Nacional 10, 2686-953 Sacavém, Portugal

[‡]Centro de Química-Física Molecular and Institute of Nanoscience and Nanotechnology, IST, Technical University of Lisbon, Avenida Rovisco Pais, 1049-001 Lisboa, Portugal

ABSTRACT: For the first time, bimetallic copper–thorium (Cu–Th–O), nickel–thorium (Ni–Th–O), and nickel–uranium (Ni–U–O) oxides were tested for the conversion of methane using N₂O as oxidant. The behavior of the uranium and thorium catalysts is very different: at 10% methane isoconversion (700 °C), the production of C₂ hydrocarbons is high over the uranium catalyst (≈80%), but the formation of oxidation products (CO₂, CO) prevails over the thorium-based catalysts (≈85 and ≈15% selectivity to CO_x and C₂). At higher temperature (750 °C), the formation of C₂ hydrocarbons remains high over the uranium catalysts (conversion CH₄ ≈ 20%, selectivity to C₂ ≈ 60%), but the production of syngas is now very high over the thorium-based catalysts (conversion CH₄ ≈ 50%, selectivity to CO and H₂ ≈ 90% at 750 °C over Ni–Th–O) without formation of C₂). This distinct behavior could not be assigned to the catalytic behavior of pure metal oxides or mechanical mixtures of single metal oxides, which is very different from that of the bimetallic oxides and was explained by the differences on the accessibility and acidity of the catalysts surface. The catalytic behavior seems to depend on the actinide element, and the catalyst can be selected accordingly with the products that we want to achieve. To our knowledge, this is the first time that the conversion of methane using N₂O as oxidant is reported over 5f block element-based catalysts.

KEYWORDS: intermetallic, bimetallic actinide oxides, methane, nitrous oxide, syngas, C₂ hydrocarbons



1. INTRODUCTION

Nitrous oxide has a much larger detrimental greenhouse effect than carbon dioxide,¹ and the decomposition of N₂O^{1–6} has been proposed as a effective method to solve an environmental problem. However, the reaction of N₂O with other products such as hydrocarbons^{7–11} or ammonia^{12,13} is not only an effective method to eliminate N₂O but also a useful chemical method to obtain value-added products. Nitrous oxide's excellent performance for some difficult oxidation processes was also recently demonstrated.²

Many efforts have been focused on the development of highly active, selective, and stable catalysts for the conversion of N₂O, and it is recognized that strong acidic catalysts are the most active ones. Strongly acidic zeolites,^{14–16} pure oxides (NiO, Co₃O₄, CoO, CuO, Fe₂O₃, SnO₂, In₂O₃, Cr₂O₃),¹⁷ mixed oxides (solid solutions, perovskites, and spinels),^{18–20} and zeolites exchanged or impregnated with transition metal ions (e.g. iron zeolites^{21–24}) are among those widely studied; however, reports on the catalytic conversion of N₂O over 5f-block element catalysts are scarce.^{25,26} To our knowledge, there are no reports on the conversion of methane using N₂O as oxidant over lanthanide- or actinide-based catalysts.

The partial oxidation of CH₄ using O₂ as oxidant as a method for the production of syngas (CO and H₂) or its use as a feedstock for the synthesis of methanol or other light

hydrocarbons has attracted a lot of attention.^{27,28} Catalysts reported to be active for the activation of methane were either noble metal- (e.g., Ir, Pt, Pd, Rh, and particularly Ru) or Ni-based compounds.²⁹ Despite the high activity of noble metal-based catalysts, they are very expensive, limiting their extensive industrial application. On the other hand, Ni-based compounds were an alternative due to their low cost. However, the major drawbacks of this reaction are the deactivation caused by sintering, changes in the oxidation state of the metal active phase, and carbon deposition.^{29–32} An alternative, the catalytic conversion of CH₄ using N₂O as the oxidant agent is a more attractive method for the elimination and valorization of two major gaseous pollutants.

In our group, we have been studying the catalytic behavior of bimetallic oxides containing f block elements using binary intermetallic compounds LnCu₂ (Ln = La, Ce, Pr, Eu, Gd, Dy, Tm),³³ LnNi (Ln = Pr, Gd, Lu), ThCu₂, and AnNi₂ (An = Th, U)³⁴ as catalytic precursors (the intermetallic route). These compounds exhibited selectivity for the 4-methylpentan-2-ol,³³ 2-propanol decomposition,³⁵ and partial oxidation of methane.^{36–38} Their activity and selectivity is clearly different from

Received: May 24, 2012

Revised: September 14, 2012

Published: October 18, 2012

that of conventional noble metal-supported catalysts on silica or alumina, and their catalytic behavior was associated with the lanthanide (actinide)-containing phase that seems to play an important role in the formation of the copper or nickel active sites. The behavior of actinide oxide-based catalysts for the partial oxidation of methane has been studied only by Choudhary³⁹ and, recently, by our group.³⁸ We have reported high methane conversion, high selectivity to syngas (H₂ and CO) at 700 °C, and good stability over bimetallic nickel- and copper-actinide oxide catalysts. These studies were performed using oxygen (or air) as oxidant. More recently, we have published some unexpected results using molten metal salts containing lanthanides as catalysts.⁴⁰

Therefore, the aim of the present study was to investigate the catalytic performance of copper-thorium, nickel-thorium, and nickel-uranium bimetallic oxides, and the reaction was investigated under different temperatures, constant GHSV, and different N₂O/CH₄ gaseous molar ratios. The catalysts were characterized before and after reaction by means of X-ray diffraction and X-ray photoelectron spectroscopy.

2. EXPERIMENTAL SECTION

2.1. Catalysts Preparation. The actinide intermetallic compounds AnNi₂ (An = Th, U) and ThCu₂ were prepared and characterized by powder X-ray diffraction and X-ray photoelectron spectroscopy (XPS) as described earlier.³⁸ Briefly, the bimetallic actinide oxides were prepared by controlled oxidation of the intermetallic compounds under air (Air Liquide, O₂/N₂ = 20:80 (vol %), purity 99.995%) at 10 °C/min heating rate up to 950 °C.³³ The pure metal oxides were used as supplied (Aldrich, purity 99.95%). The mechanical mixtures were prepared prior to use on an agate crucible using a MO/AnO₂ or ₃ (M = Cu, Ni, and An = Th, U) molar ratio of 2.

2.2. Catalysts Characterization. Specific surface areas (BET) were determined in a volumetric automatic apparatus (Quantacrome, Nova 2200e) at -196 °C using a liquid nitrogen cryogenic bath (Air Liquid, 99.999%). The samples, between 100 and 1000 mg, were degassed for 2.5 h at a pressure lower than 0.133 Pa. The degassing temperature was 150 °C for all samples. The values obtained were for all catalysts below 1 m²/g.

Powder X-ray diffraction (XRD) patterns were obtained with a PANalytical X'Pert Pro diffractometer using monochromatized Cu K_α radiation ($\lambda = 1.5406 \text{ \AA}$). The operational settings for all scans were voltage = 45 kV, current = 40 mA, and 2θ scan range 5–80° using a step size of 0.03° at a scan speed of 0.02°/min. For identification purposes, the relative intensities (I/I_0) and the d spacing (\AA) were compared with standard JCPDS powder diffraction files.⁴¹

The XPS measurements were performed in a spectrometer XSAM800 (KRATOS) under a vacuum greater than 10⁻⁶ Pa. Nonmonochromatic Al K_α radiation (main line at 1486.6 eV) operated at 120 W (10 mA × 12 kV) and pass energy = 20 eV was used. Data treatment was performed as described earlier.³⁸ For quantification purposes, the sensitivity factors were 0.66 for O 1s, 0.25 for C 1s, 4.16 for Cu 2p_{3/2}, 3.53 for Ni 2p_{3/2}, 5.76 for Th 4f_{7/2}, and 11.23 for U 4f.

2.3. Catalytic Activity. The catalytic partial oxidation of methane was carried out at atmospheric pressure in a fixed-bed U-shaped quartz reactor, plug-flow type reactor, with a quartz frit and an inside volume of 15 cm³. The reactor was kept in a tubular furnace. Mass flow controllers were used to control CH₄ (Air Liquide, purity 99.9995%), N₂O (Air Liquide, purity

99.9995%), and He (Air Liquide, purity 99.9995%) flows. A thermocouple was placed on the catalytic bed for continuous monitoring of the sample temperature. Unless otherwise stated, a gaseous mixture of CH₄ (3%), N₂O (3%), and He (94%) was introduced, and the reaction was studied with an adequate gas hourly space velocity (GHSV = 8500 mL of CH₄/g of catalyst·h). The amount of sample ($\approx 20 \text{ mg}$) was selected in such a way that rate limitation by external mass and heat transport processes under differential conditions proved to be negligible by applying suitable experimental criteria, such as those defined by Froment and Bischoff⁴² ($\Delta P_{\text{CH}_4} < 1 \times 10^{-4} \text{ atm}$; $(\Delta T)_{\text{max}} < 1 \text{ K}$). Since the catalysts are nonporous solids, the study of the influence of pore diffusion on the reaction rate (Weisz-Prater criterion) was not undertaken. The outlet gas was first cooled in an ice water trap prior to analysis. The decomposition of N₂O was studied under the same conditions using a gaseous mixture of N₂O (3%) and He (97%). The outlet gas composition was analyzed online by gas chromatography using a Restek ShinCarbon ST column ($L = 2.0 \text{ m}$, $\phi = 1/8 \text{ in.}$, i.d. = 1 mm, 100/200 mesh) and an Agilent 4890D GC equipped with a thermal conductivity detector (carrier gas He (10 mL/min) and a two-ramp temperature program (oven temperature was held at 35 °C for 5 min, then programmed from 35 to 100 °C at 10 °C/min for the first ramp. The oven temperature was held at 100 °C for 32 min, then programmed from 100 to 250 °C at 40 °C/min for the second ramp, then held at 250 °C for 10 min before cool-down to 35 °C) and a 6-port gas sampling valve with a 0.250 μL loop. The quantification of reagents and products was confirmed by an external standard method using reference mixtures of H₂, N₂, O₂, CO, CO₂, CH₄, C₂H₄, C₂H₆, C₃H₆ (propene), C₃H₈ (propane), C₄H₆ (1,3-butadiene), C₄H₈ (1-butene, 2-butene), and C₄H₁₀ (butane, isobutane) (AirLiquide). Catalyst activity was defined as the number of milliliters of methane converted per gram of catalyst and per hour (mL CH₄/g h⁻¹). The conversion of methane, the selectivity, and the yield of the products were calculated as described elsewhere.³⁸ The confidence level was >95%. Unless otherwise stated, the values reported in this paper represent the initial activities of the catalysts after 1 h on-stream.

3. RESULTS AND DISCUSSION

The bimetallic actinide oxides were active and selective for the conversion of methane using N₂O as oxidant. Figures 1 and 2 show the effect of the temperature on their activity and selectivity (range studied 650–800 °C). A brief study performed at 700 °C without catalyst (blank test, results not shown) confirms that the contribution of the conversion of N₂O and CH₄ are irrelevant (<1%). For comparison purposes, a study over pure metal oxides was also undertaken. Pure NiO and the thorium bimetallic oxide catalysts—namely, nickel-thorium bimetallic oxide catalyst—present the highest activity (conversion of CH₄ $\approx 70\%$ at $T \geq 750 \text{ °C}$) (Figure 1).

The reaction main products were H₂, CO, CO₂, and C₂ hydrocarbons (C₂H₄ and C₂H₆). The formation of O₂ was never detected. The absence of O₂ in the gas phase in the experiments is not surprising because CH₄ reacts with adsorbed oxygen species formed from N₂O, and because of the fast consumption of these species, O₂ cannot be observed.^{43,44} The production of H₂ and CO increases with the temperature (Figure 2a and b), and the best results for the production of syngas were those obtained over the thorium-based catalysts,

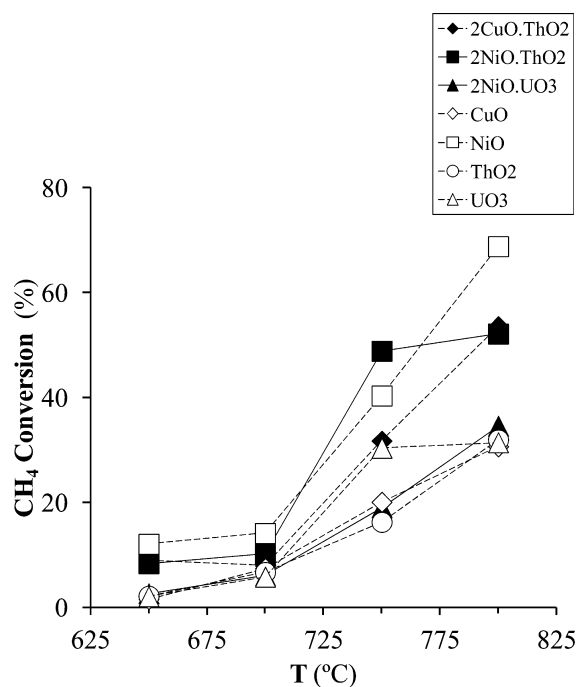


Figure 1. Effect of the temperature on the conversion of methane.

especially over $2\text{Ni}\cdot\text{ThO}_2$ at $T \geq 750\text{ }^\circ\text{C}$ (selectivity to CO and $\text{H}_2 \sim 90\%$, with low production of C_2 hydrocarbons $\leq 4\%$), and NiO . On the other hand, over the nickel–uranium bimetallic oxide catalyst ($2\text{NiO}\cdot\text{UO}_3$) and over pure ThO_2 , the main products were C_2 hydrocarbons (selectivity $\sim 70\text{--}80\%$ at $700\text{ }^\circ\text{C}$ that decreases with the temperature) (Figure 2c). Therefore, it can be concluded that the catalytic behavior of the nickel-based catalysts seems to depend on the actinide element, which makes possible a catalyst selection accordingly with the product that we want to obtain.

To confirm the hypothesis, their catalytic behavior for the production of hydrocarbons was studied at $700\text{ }^\circ\text{C}$, and the results were compared at $\approx 8\%$ isoconversion (Figure 3). Clearly, the selectivity depends on the type of catalyst and confirms our previous statement.

Concerning the behavior of the pure metal oxides, they give rise to high production of C_2 hydrocarbons over ThO_2 and UO_3 and a high selectivity to syngas over NiO . On the basis of this observation (Figure 3), we can assume that UO_3 is the main active phase on $2\text{NiO}\cdot\text{UO}_3$. In terms of thorium-based compounds, their results are better explained if we consider that the main active phase is due to the pure metal d oxide phases (CuO or NiO) rather than that of ThO_2 .

A comparison of the mechanical mixtures of pure metal oxides with the bimetallic copper- and nickel–actinide oxides was done. The formation of hydrogen was never observed over MM of pure metal oxides, even at $T \geq 750\text{ }^\circ\text{C}$. As an example, for $750\text{ }^\circ\text{C}$ with a $\approx 15\%$ isoconversion, the $2\text{NiO}\cdot\text{UO}_3$ shows 60% C_2 hydrocarbon selectivity against 40% for the mechanical mixture $2\text{NiO}/\text{UO}_3$. Such a result reinforces that we are dealing with bimetallic oxides and not a simple mixture of oxides.

Moreover, the catalytic behavior of the bimetallic actinide oxides is influenced by the $\text{N}_2\text{O}/\text{CH}_4$ gaseous molar feed ratio (range 1–8) that increases the conversion of CH_4 (Figure 4) and the selectivity to CO_x (for the latter, data not shown). In contrast, it has a negative influence on the selectivity to hydrocarbons (Figure 5), except for NiO and $\text{Ni}\text{--}\text{Th}\text{--}\text{O}$

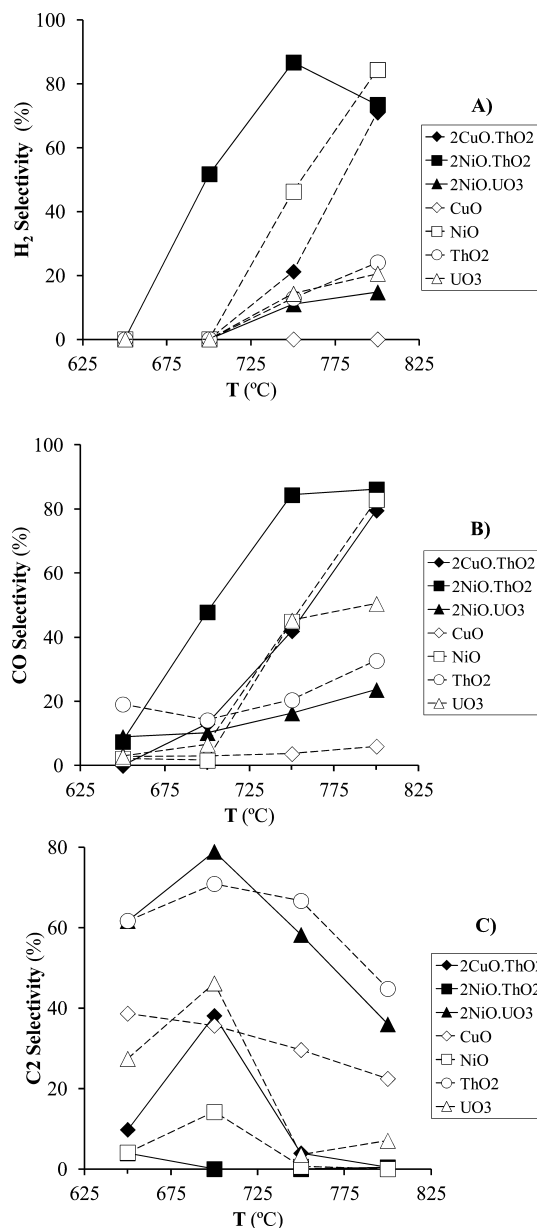


Figure 2. Effect of the temperature on the selectivity to (A) H_2 , (B) CO , and (C) C_2 hydrocarbons.

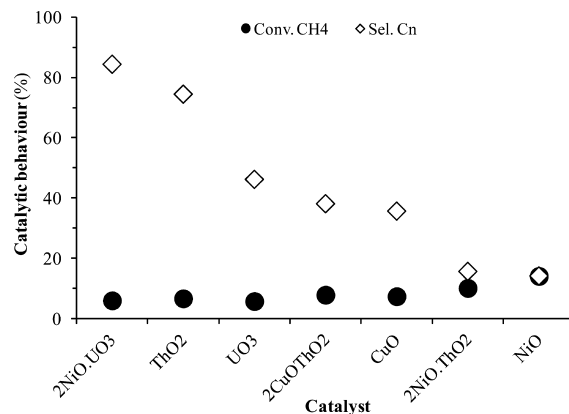


Figure 3. Catalytic behavior over pure metal oxides and bimetallic oxides catalysts at $700\text{ }^\circ\text{C}$.

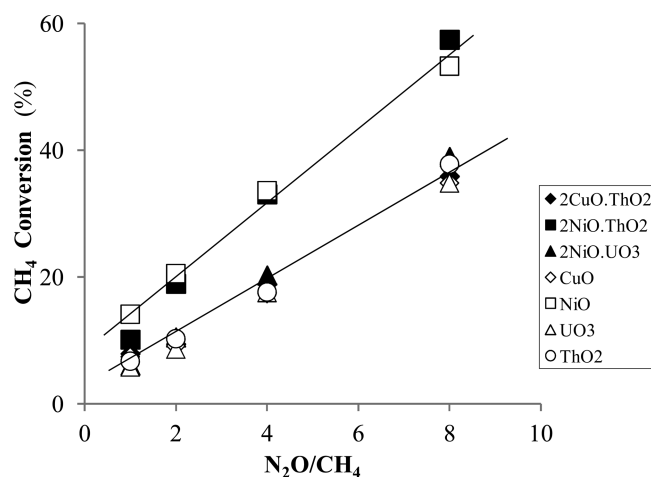


Figure 4. $\text{N}_2\text{O}/\text{CH}_4$ molar feed ratio effect on the catalysts' activity at 700 °C.

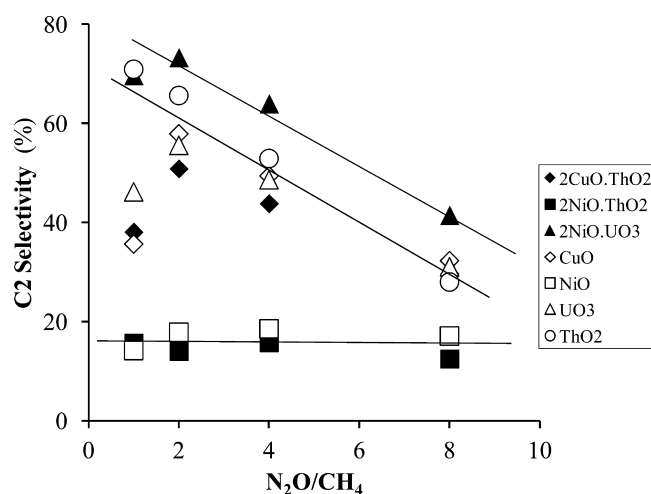


Figure 5. $\text{N}_2\text{O}/\text{CH}_4$ molar feed ratio effect on the catalysts' selectivity to C2 hydrocarbons at 700 °C.

catalysts. The values depicted in Figures 4 and 5 represent two sets of values obtained at isoconversion, one for NiO and 2NiO·ThO₂ and the other one for the rest of the catalysts. Over the first group of catalysts, the selectivity to C2 hydrocarbons is very low (the lowest values measured in this study), and it is not influenced by the $\text{N}_2\text{O}/\text{CH}_4$ gaseous molar feed ratio (a possible explanation will be given later). Over all the other catalysts, the highest values for the production of hydrocarbons were those obtained over 2NiO·UO₃ and ThO₂.

Finally, if we compare the data previously obtained over the bimetallic copper– and nickel–actinide oxides (Th, U) for the conversion of methane using O₂ as oxidant,³⁸ the results obtained now under N₂O are clearly different, and the activity over the bimetallic nickel–actinide oxide catalysts (Ni–An–O, An = Th, U) is to a large extent higher under O₂ than under N₂O, except for the bimetallic copper–thorium oxide catalyst (2CuO·ThO₂) (Figure 6).

The selectivity follows also a distinct pattern: syngas (H₂ and CO) is formed mainly under O₂, whereas C2 hydrocarbons were obtained mainly under N₂O, particularly over the bimetallic nickel–uranium (Ni–U–O) catalyst (Figure 7). Such catalysts present the highest selectivity toward C2 measured in this work ($\approx 85\%$). The results obtained with

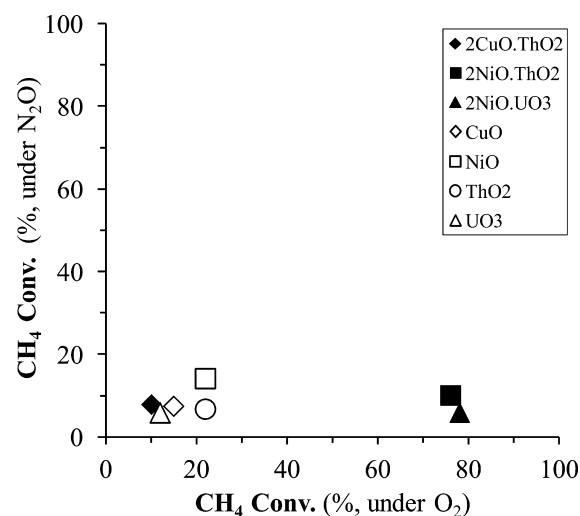


Figure 6. Effect of oxidant on the conversion of methane at 700 °C.

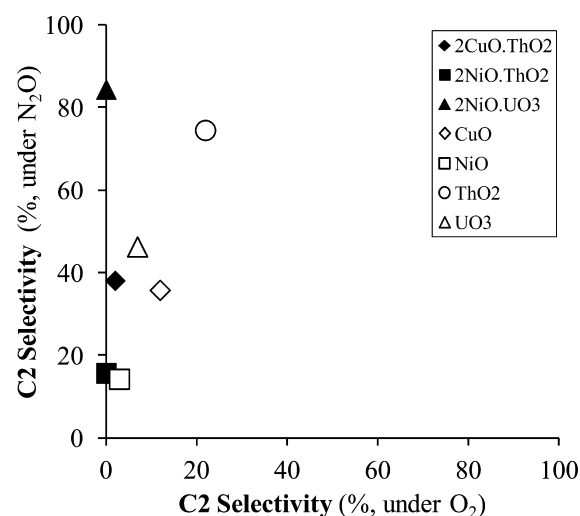


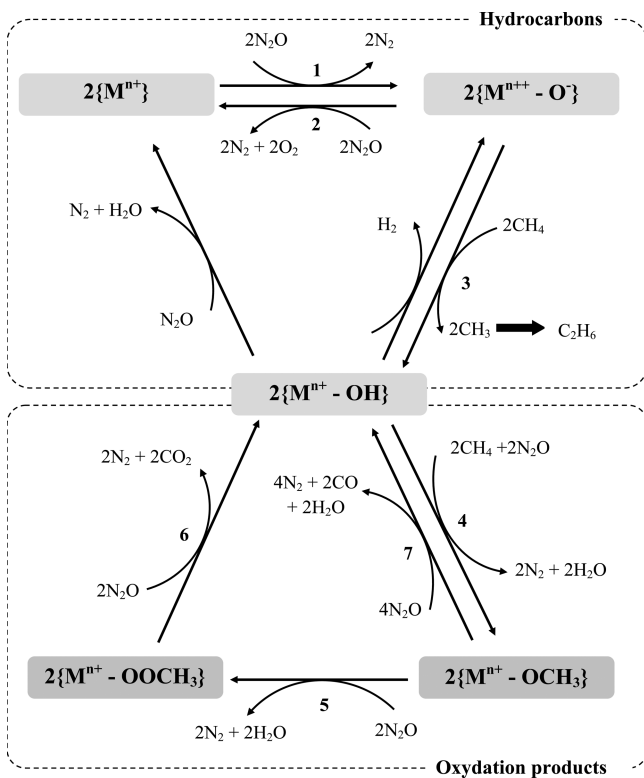
Figure 7. Effect of the oxidant on the selectivity to C2 hydrocarbons at 700 °C.

pure actinide oxides are also good; namely, the behavior of ThO₂ and UO₃ for the production of C2 hydrocarbons and syngas (Figures 2 and 3) under N₂O, respectively. Nevertheless, it is clear that the reaction under O₂ favors the formation of syngas and oxidation products, whereas the conversion of CH₄ under N₂O favors the formation of hydrocarbons.

To better explain our results for the activation of CH₄ with N₂O, we propose the following mechanism, in agreement with results already published.^{43,45–51} The decomposition of nitrous oxide is a simple reaction that produces only nitrogen and oxygen in the expected stoichiometric ratio (1:0.5). The conversion of N₂O can proceed by two parallel routes either with the formation of molecular oxygen or toward the formation of acidic sites, for example, single vacancy oxygen species (O[−]). If the reaction follows the first route, the results are very similar to the ones obtained when the reaction is carried on with O₂. If the reaction follows the second route, the acidic sites will be responsible for the conversion of methane and formation of CH₃ radicals and ethane as a coupling product.^{45–47} Accordingly, the first step of the reaction is the adsorption of N₂O on the catalyst, which implies the oxidation

of the catalyst (mechanism I, reaction 1; N_2O decomposition over oxygen vacancies). The second step consists of the reaction of the oxidized site with another N_2O molecule (mechanism I, reaction 2) and restores the initial state of (M^{n+}) .^{47–49}

Scheme 1. Mechanism I



The key issue for the activation of N_2O seems to be the reactivity of the vacancy oxygen species rather than the excess concentration of adsorbed oxygen.^{50,52,53} The formation of these very short lifetime (shorter than 100 ms) anion radical oxygen species (called α -oxygen that we describe as $\{(M^{n+})-O^-\}$), with low binding energy to the surface, and highly reactive, is essential to explain the formation of all the products detected in this work during the catalytic activation of CH_4 by N_2O .

It has been demonstrated that the behavior of these vacancies oxygen species implies their activation in situ and the coexistence with N_2O in the gas phase for a successful CH_4 activation,⁴⁷ which confirm the importance of the $\text{N}_2\text{O}/\text{CH}_4$ molar feed ratio and the main formation of oxidation products under an excess of N_2O ($\text{N}_2\text{O}/\text{CH}_4 > 1$). The oxygen species give rise to the formation of the surface hydroxides, which are directly linked with the catalyst activity and selectivity. The presence and stability of surface hydroxides at high temperatures (>700 °C) is a known fact from the literature and allows us to state their importance on the reaction mechanism.^{54–56}

In fact, the formation of CO_2 involves a quick transformation of surface hydroxides into surface alkoxides that react with other N_2O molecules (mechanism I, reactions 3–6), whereas the formation of CO is explained if reaction 7 replaces reactions 5 and 6.⁵¹ Such reactions become thermodynamically more favorable with the increase in the concentration of N_2O in the gas phase, which also explains the decrease in the C2 hydrocarbons with the $\text{N}_2\text{O}/\text{CH}_4$ gaseous molar feed ratio

(Figure 5). In the case of H_2 formation, that appears only if CO or CO_2 is also detected in the gas phase. This can be explained by the transformation of the surface hydroxide species $2\{(M^{n+})-OH\}$ into $\{(M^{n+})-O^-\} + \text{H}_2$ that is enhanced by the increasing concentration of such species on the catalysts' surface.

Therefore, it can be said that the proposed mechanism I explains the formation of all products and the effect of the experimental conditions on the reaction selectivity, but to explain the differences observed (e.g. when uranium replaces thorium on the nickel catalyst), the catalysts' surface analysis by XRD and XPS was also undertaken. The catalysts' XRD patterns obtained before reaction were consistent with those reported earlier by our group³⁴ and show only the diffraction patterns of NiO , CuO , ThO_2 , and UO_3 cubic phases, as reported in the standard JCPDS powder diffraction files.⁴¹ After reaction, the XRD diffraction patterns are similar under either N_2O or O_2 , and the formation of oxide phases that could correspond to the formation of new solid solutions between CuO/NiO and the actinide oxide phase was not detected (Figure 8). However, metallic Ni and Cu due to nickel and

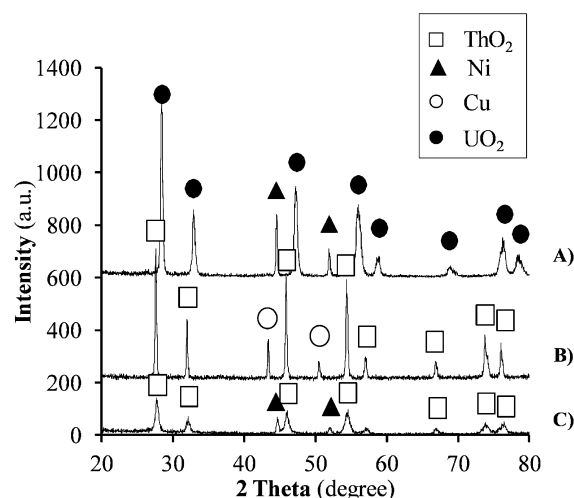


Figure 8. XRD patterns obtained after reaction for the bimetallic actinide oxides: (A) $2\text{NiO}\cdot\text{UO}_3$, (B) $2\text{CuO}\cdot\text{ThO}_2$, and (C) $2\text{NiO}\cdot\text{ThO}_2$.

copper oxide total reduction were identified by XRD. In the case of the nickel–uranium bimetallic oxide, the reduction of UO_3 to UO_2 could also be identified. Therefore, the analysis of the catalysts by XRD reveals some modifications on the catalysts; namely, the reduction of copper and uranium and the coexistence of oxidized and partially reduced phases that could be linked to the formation of C2 hydrocarbons over the $\text{Cu}\text{--}\text{Th}\text{--}\text{O}$ and $\text{Ni}\text{--}\text{U}\text{--}\text{O}$ catalysts.

Table 1 shows the XPS data obtained after reaction. Before reaction, the spectra were already presented in a previous paper.³⁸ From a quantitative point of view, the actinide/metal ratio slightly decreases for $\text{Cu}\text{--}\text{Th}\text{--}\text{O}$ and increases for the nickel-based compounds ($\text{Ni}\text{--}\text{Th}\text{--}\text{O}$ and $\text{Ni}\text{--}\text{U}\text{--}\text{O}$).

The $\text{Ni}\text{--}\text{Th}\text{--}\text{O}$ catalyst behavior is very similar to the one in the presence of O_2 : because of the large amount of carbon after reaction, $\text{Th } 4f_{7/2}$ and, in particular, $\text{Ni } 2p_{3/2}$ XPS photoelectrons are strongly attenuated by a carbonaceous overlayer, making the analysis very difficult. This carbonaceous contamination is, in principle, a consequence of the catalyst higher

Table 1. Relative Atomic Amounts and Atomic Ratios before (BR) and after (AR) Reaction at 800 °C

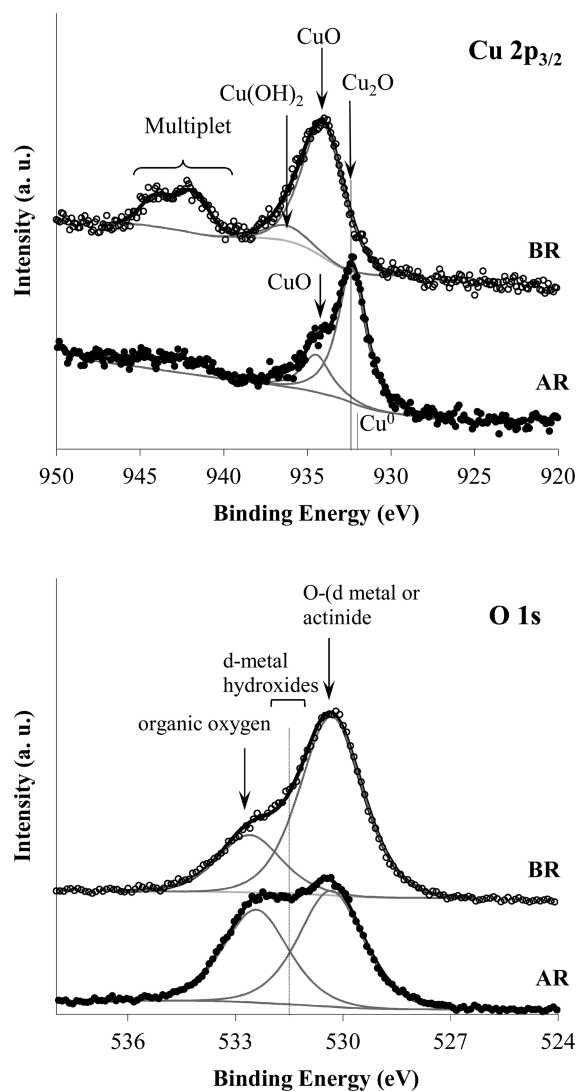
	at. concn %					
	Cu–Th oxides		Ni–Th oxides		Ni–U oxides	
	BR	AR	BR	AR	BR	AR
C	21.9	35.1	18.8	87.6	27.2	65.1
O	56.9	48.9	56.2	10.3	50.8	30.7
Th	11.8	8.1	14.4	1.8		
Cu	9.4	7.1				
Ni			10.5	0.3	10.5	0.9
U					6.7	3.4
C/An	1.9	4.3	1.3	48.9	4.0	19.5
An/Cu or Ni	1.3	1.1	1.4	5.3	0.6	3.8

activity that leads to the formation of CO and H₂ and could also be responsible for the absence of an N₂O/CH₄ molar feed rate effect on the catalyst selectivity (Figure 5).

The increase in CH₄ conversion with the N₂O/CH₄ molar feed ratio indicates that the number of oxygen species required for methane activation also increases (Figure 4). Nevertheless, no molecular oxygen was detected in the gaseous effluent during the catalytic studies, which is a surprise in the presence of N₂O at high temperatures (>650 °C). Zhu et al.⁵⁷ attributed such behavior to the high reactivity of such molecular oxygen, which increases the conversion of CH₄ into products not detected during the catalytic study (e.g. coke and H₂O⁵⁴), leading to an insignificant variation of the selectivity with the increase in the N₂O/CH₄ molar feed ratio, as observed for NiO and Ni–Th–O (Figure 5). In the case of the bimetallic nickel–thorium oxide, such a hypothesis is supported by the huge increase in the carbon detected after reaction by XPS. Loughran¹⁶ reported a similar result for the conversion of NO and CH₄ over Pd/ZSM-5.

However, relative to our previously reported results for the partial oxidation of methane,³⁸ after reaction, the main differences in the XPS arise from the Ni–U–O and Cu–Th–O catalysts (those that produce hydrocarbons). The photoelectron attenuation due to a carbonaceous overlayer is not so dramatic in the Ni–U–O system, allowing the detection of quantitative changes in the nickel oxide/hydroxide species at the surface. Before reaction, the Ni 2p_{3/2} regions (not shown) of nickel-based catalysts are a composition of oxides and hydroxides with peak maxima centered at 854.2, 855.1, and 856.0 (±0.2) eV assigned to NiO, Ni(OH)₂, and NiOOH, respectively.⁵⁸ After reaction, a new component centered at a lower binding energy (852.8 ± 0.2 eV), corresponding to Ni⁰, is also present. In Cu–Th–O, the Cu 2p region is very different from before the reaction. It is also very different from the same region in the after-reaction sample in the presence of O₂.³⁸

Figure 9 shows the Cu 2p_{3/2} and O 1s regions for both samples before and after reaction in the presence of N₂O. Before reaction, copper is mainly in the form of Cu²⁺, (CuO and Cu(OH)₂), as attested by the presence of a multiplet structure (between 940 and 945 eV) characteristic of Cu²⁺ species. After reaction, copper is partially reduced: the main peak was shifted to 932.3 eV, a binding energy typical of Cu⁺ or Cu⁰, and the multiplet structure is less intense. However, the computed Auger parameter (AP(Cu 2p_{3/2}, Cu L₃M₄₅M₄₅) = 1849.5)⁵⁹ shows undoubtedly that, after reaction, the main peak in Cu 2p_{3/2} is Cu⁺ and not Cu⁰. Moreover, after reaction, the amount of copper hydroxides is residual. Taking into account that after reaction, the exposure of the catalyst to the

**Figure 9.** Copper–thorium bimetallic oxide Cu–Th–O: Cu 2p_{3/2} and O 1s XPS regions before reaction (BR) and after reaction (AR).

atmosphere may reoxidize its surface, the results here described show that the reoxidation, if any, is far from being complete, since an overall decrease in the oxidation state for d metals is detected. The carbonaceous layer formed during the reaction is probably a barrier for the oxygen diffusion to reach the catalyst surface.

Concerning the oxygen species bound to the d metals, quantitative results are shown in Table 2. As relevant information, it is very clear that for the reaction under N₂O, the relative amount of d metal bound to OH groups (atomic ratios: (d metal bound to OH)/(total d metal), computed from Cu 2p_{3/2} or Ni 2p_{3/2} XPS regions) decreases during reaction. In contrast, under O₂, the relative amount of d metal bound to OH groups increases during reaction (increase of catalyst oxidant strength), which supports the observed selective formation of oxidation products or syngas reported before.³⁸

It is known that the amount and accessibility of surface hydroxide species can be directly linked to the catalysts acidity, which is a main factor that governs the catalyst activity and selectivity. Miller et al.¹⁵ studied the role of acid sites in cobalt zeolite catalysts for selective catalytic reduction of NO_x and found a direct correlation between the increase in the number

Table 2. Relative Amounts of Oxygen Species Bound to the Metals

atomic ratio	catalyst								
	Cu–Th oxides			Ni–Th oxides			Ni–U oxides		
	BR	AR		BR	AR		BR	AR	
		O ₂	N ₂ O		O ₂	N ₂ O		O ₂	N ₂ O
d metal–OH/total d metal	0.2	0.7	0.0	0.4	1.0	0.4	0.7	1.0	0.6
O _{total} /d metal	4.3	6.5	6.9	5.4	12.9	30.3	8.2	4.0	34.8
O _{total} /An	4.7	4.0	6.0	3.5	3.3	5.7	7.6	8.3	9.2

of acid sites and the catalysts' activity for the decomposition of NO_x. Therefore, the disappearance of the surface hydroxides in the case of the conversion of methane under N₂O could explain the lower activity of the Cu–Th–O catalyst.

In contrast, over the nickel-based compounds and despite the nickel XPS signal attenuation due to a graphitization effect of the catalysts' extreme surface with the reaction under N₂O, hydroxide species are still detected. The highest activity observed for these compounds is certainly related to the presence of these hydroxide groups. In the particular case of Ni–U–O, the carbonaceous overlayer seems to be not as thick as in the Ni–Th–O system (cf. the relative amount of carbon in Table 1), allowing for larger accessibility to acid sites over the Ni–U–O catalyst. This correlates to the higher selectivity to C₂ hydrocarbons detected over such catalysts. Over the Ni–Th–O catalyst, the formation of large carbonaceous deposits limits the accessibility, enhancing the formation of oxidation products.¹⁶

The existence of a synergism between nickel and actinides is also a factor that could influence the bimetallic actinide oxides' selectivity.^{34,36,38,60} It is known that there is a donation of electrons from the actinide to nickel that is larger on thorium catalysts than on those with uranium.^{38,60} This implies a nickel electrophile character larger on Ni–Th–O than on Ni–U–O that could facilitate the formation and stabilization of alkyl radicals by hydrogen abstraction over Ni–U–O. Consequently, it renders easier the formation of ethane after the activation and dimerization of methane (a mechanism widely accepted) on the uranium catalyst. For that reason, Panov et al.⁶¹ proposed hydrogen abstraction as the initial step of the reaction (mechanism I, reaction 3) yielding methyl radicals that are quickly transformed into surface hydroxides with the formation of ethane or ethylene by the subsequent dehydrogenation of ethane. However, further work is needed to confirm such a hypothesis.

4. CONCLUSIONS

The results reported in this article show that the bimetallic copper– and nickel–actinide oxides obtained by an intermetallic route via oxidation of UNi₂ and ThM₂ (M = Cu, Ni) were active and selective for the conversion of methane using N₂O as oxidant. The Ni–U–O oxide catalyst was very active and selective for production of C₂ hydrocarbons, whereas the bimetallic Ni–Th–O oxide catalyst was very active and selective for the production of synthesis gas. The catalytic performance increases when Ni replaces Cu, and Cu–Th–O always presented the lowest activity and selectivity toward hydrocarbons. The catalytic differences between the nickel-based compounds were explained in terms of (i) worse accessibility to the surface of Ni–Th–O because of the formation of a huge carbonaceous overlayer that is a consequence of the catalyst higher activity for the formation

of oxidation products instead of hydrocarbons and (ii) an electrophile character that is larger on Ni–Th–O than on Ni–U–O that could facilitate the formation and stabilization of alkyl radicals by hydrogen abstraction and, consequently, facilitate the formation of ethane. The higher activity of the nickel–actinide catalyst has been attributed to its acidity, which is a main factor that governs the catalyst activity and selectivity. To our knowledge, this is the first time that the conversion of methane using nitrous oxide as oxidant for the production of either syngas or C₂ hydrocarbons has been reported over 5f block element-based catalysts.

AUTHOR INFORMATION

Corresponding Author

*Phone: +351.219946116. Fax: +351.219941455. E-mail: jbranco@itn.pt.

Notes

The authors declare no competing financial interest.

ACKNOWLEDGMENTS

This work was supported by the Portuguese “Fundação para a Ciência e a Tecnologia” under Contract PTDC/EQU-EQU/65126/2006. Ana C. Ferreira thanks FCT for her Ph.D. grant (SFRH/BD/69942/2010). Ana M. Ferraria thanks FCT for a postdoctoral grant (SFRH/BPD/26239/2006).

REFERENCES

- (1) Kapteijn, F.; Rodriguez Mirasol, J.; Moulijn, J. A. *Appl. Catal., B* **1996**, *9* (1–4), 25–64.
- (2) Boissel, V.; Tahir, S.; Koh, C. A. *Appl. Catal., B* **2006**, *64* (3–4), 234–242.
- (3) Gervasini, A.; Carniti, P.; Bennici, S. *React. Kinet. Mech. Catal.* **2012**, *105* (1), 53–67.
- (4) Daquin, J. P.; Dujardin, C.; Granger, P. *Catal. Today* **2008**, *137* (2–4), 390–396.
- (5) Shen, Q.; Li, L. D.; Li, J. J.; Tian, H.; Hao, Z. P. *J. Hazard. Mater.* **2009**, *163* (2–3), 1332–1337.
- (6) Wang, Y. H.; Zhang, J. C.; Zhu, J. L.; Yin, J. M.; Wang, H. M. *Energy Convers. Manage.* **2009**, *50* (5), 1304–1307.
- (7) Nobukawa, T.; Kita, K.; Tanaka, S.; Ito, S.; Miyadera, T.; Kameoka, S.; Tomishige, K.; Kunimori, K. *Stud. Surf. Sci. Catal.* **2002**, *142*, 557–564.
- (8) Borko, L.; Koppány, Z.; Schay, Z.; Guzzi, L. *Catal. Today* **2009**, *143* (3–4), 269–273.
- (9) Nobukawa, T.; Yoshida, M.; Kameoka, S.; Ito, S.; Tomishige, K.; Kunimori, K. *Stud. Surf. Sci. Catal.* **2004**, *154*, 2514–2521.
- (10) Nobukawa, T.; Yoshida, M.; Kameoka, S.; Ito, S. I.; Tomishige, K.; Kunimori, K. *Catal. Today* **2004**, *93–95*, 791–796.
- (11) Van den Brink, R. W.; Booneveld, S.; Pels, J. R.; Bakker, D. F.; Verhaak, M. J. F. M. *Appl. Catal., B* **2001**, *32* (1–2), 73–81.
- (12) Delahay, G.; Mauvezin, M.; Coq, B.; Kieger, S. *J. Catal.* **2001**, *202* (1), 156–162.
- (13) Delahay, G.; Mauvezin, M.; Guzman-Vargas, A.; Coq, B. *Catal. Commun.* **2002**, *3* (8), 385–389.

- (14) Petunchi, J. O.; Hall, W. K. *Appl. Catal., B* **1993**, *2* (2–3), L17–L26.
- (15) Miller, J. T.; Glusker, E.; Peddi, R.; Zheng, T.; Regalbutto, J. R. *Catal. Lett.* **1998**, *51* (1–2), 15–22.
- (16) Loughran, C. J.; Resasco, D. E. *Appl. Catal., B* **1995**, *5* (4), 351–365.
- (17) Satsuma, A.; Maeshima, H.; Watanabe, K.; Suzuki, K.; Hattori, T. *Catal. Today* **2000**, *63* (2–4), 347–353.
- (18) Alini, S.; Basile, F.; Blasioli, S.; Rinaldi, C.; Vaccari, A. *Appl. Catal., B* **2007**, *70* (1–4), 323–329.
- (19) Russo, N.; Mescia, D.; Fino, D.; Saracco, G.; Specchia, V. *Ind. Eng. Chem. Res.* **2007**, *46* (12), 4226–4231.
- (20) Santiago, M.; Perez-Ramirez, J. *Environ. Sci. Technol.* **2007**, *41* (5), 1704–1709.
- (21) Kondratenko, E. V.; Perez-Ramirez, J. *J. Phys. Chem. B* **2006**, *110* (45), 22586–22595.
- (22) Li, L. D.; Shen, Q.; Yu, J. J.; Hao, Z. P.; Xu, Z. P.; Lu, G. Q. *Environ. Sci. Technol.* **2007**, *41* (22), 7901–7906.
- (23) Pieterse, J. A. Z.; Booneveld, S.; van den Brink, R. W. *Appl. Catal., B* **2004**, *51* (4), 215–228.
- (24) Pirngruber, G. D. *J. Catal.* **2003**, *219* (2), 456–463.
- (25) Ivanov, D. V.; Sadovskaya, E. M.; Pinaeva, L. G.; Isupova, L. A. *J. Catal.* **2009**, *267* (1), 5–13.
- (26) Satsuma, A.; Maeshima, H.; Watanabe, K.; Hattori, T. *Energy Convers. Manage.* **2001**, *42* (15–17), 1997–2003.
- (27) Alvarez-Galvan, M. C.; Mota, N.; Ojeda, M.; Rojas, S.; Navarro, R. M.; Fierro, J. L. G. *Catal. Today* **2011**, *171* (1), 15–23.
- (28) Aasberg-Petersen, K.; Dybkjær, I.; Ovesen, C. V.; Schjødt, N. C.; Sehested, J.; Thomsen, S. G. *J. Nat. Gas Sci. Eng.* **2011**, *3* (2), 423–459.
- (29) Enger, B. C.; Lodeng, R.; Holmen, A. *Appl. Catal., A* **2008**, *346* (1–2), 1–27.
- (30) Mateos-Pedrero, C.; Cellier, C.; Eloy, P.; Ruiz, P. *Catal. Today* **2007**, *128* (3–4), 216–222.
- (31) Li, J. M.; Huang, F. Y.; Weng, W. Z.; Pei, X. Q.; Luo, C. R.; Lin, H. Q.; Huang, C. J.; Wan, H. L. *Catal. Today* **2008**, *131* (1–4), 179–187.
- (32) York, A. P. E.; Xiao, T. C.; Green, M. L. H. *Top. Catal.* **2003**, *22* (3–4), 345–358.
- (33) Ballivet-Tkatchenko, D.; Branco, J.; Dematos, A. P. *J. Phys. Chem.* **1995**, *99* (15), 5481–5484.
- (34) Branco, J.; de Jesus Dias, C.; Goncalves, A. P.; Gasche, T. A.; de Matos, A. P. *Thermochim. Acta* **2004**, *420* (1–2), 169–173.
- (35) Branco, J. B.; Dias, C. J.; Goncalves, A. P. *J. Alloys Compd.* **2009**, *478* (1–2), 687–693.
- (36) Ferreira, A. C.; Ferrara, A. M.; do Rego, A. M. B.; Goncalves, A. P.; Correia, M. R.; Gasche, T. A.; Branco, J. B. *J. Alloys Compd.* **2010**, *489* (1), 316–323.
- (37) Ferreira, A. C.; Ferrara, A. M.; do Rego, A. M. B.; Goncalves, A. P.; Girao, A. V.; Correia, R.; Gasche, T. A.; Branco, J. B. *J. Mol. Catal. A: Chem.* **2010**, *320* (1–2), 47–55.
- (38) Ferreira, A. C.; Goncalves, A. P.; Gasche, T. A.; Ferrara, A. M.; do Rego, A. M. B.; Correia, M. R.; Bola, A. M.; Branco, J. B. *J. Alloys Compd.* **2010**, *497* (1–2), 249–258.
- (39) Choudhary, V. R.; Rajput, A. M.; Prabhakar, B.; Mamman, A. S. *Fuel* **1998**, *77* (15), 1803–1807.
- (40) Branco, J. B.; Lopes, G.; Ferreira, A. C. *Catal. Commun.* **2011**, *12*, 1425–1427.
- (41) JCPDS. *The Powder Diffraction File*; JCPDS: 1601 Park Avenue, Swarthmore, PA, 1981.
- (42) Froment, G. F.; Bischoff, K. B., *Chemical Reactor Analysis and Design*; John Wiley & Sons: New York, 1979.
- (43) Otsuka, K.; Nakajima, T. *J. Chem. Soc., Faraday Trans. 1* **1987**, *83* (4), 1315–1321.
- (44) Kondratenko, V. A.; Hahn, T.; Kondratenko, E. V. *ChemCatChem* **2012**, *4* (3), 408–414.
- (45) Anshits, A. G.; Kondratenko, E. V.; Voskresenskaya, E. N.; Kurteeva, L. I.; Pavlenko, N. I. *Catal. Today* **1998**, *46* (2–3), 211–216.
- (46) Vereshchagin, S. N.; Kirik, N. P.; Shishkina, N. N.; Morozov, S. V.; Vyalkov, A. I.; Anshits, A. G. *Catal. Today* **2000**, *61* (1–4), 129–136.
- (47) Nobukawa, T.; Sugawara, K.; Okumura, K.; Tomishige, K.; Kunimori, K. *Appl. Catal., B* **2007**, *70* (1–4), 342–352.
- (48) Pirutko, L. V.; Chernyavsky, V. S.; Starokon, E. V.; Ivanov, A. A.; Kharitonov, A. S.; Panov, G. I. *Appl. Catal., B* **2009**, *91* (1–2), 174–179.
- (49) Kondratenko, E. V.; Perez-Ramirez, J. *Catal. Today* **2007**, *119* (1–4), 243–246.
- (50) Centi, G.; Dall’Olio, L.; Perathoner, S. *J. Catal.* **2000**, *194* (1), 130–139.
- (51) Shen, Q.; Li, L. D.; He, C.; Tian, H.; Hao, Z. P.; Xu, Z. P. *Appl. Catal., B* **2009**, *91* (1–2), 262–268.
- (52) Perez-Ramirez, J.; Kapteijn, F.; Mul, G.; Moulijn, J. A. *J. Catal.* **2002**, *208* (1), 211–223.
- (53) Tanaka, S.; Yuzaki, K.; Ito, S.; Kameoka, S.; Kunimori, K. *J. Catal.* **2001**, *200* (2), 203–208.
- (54) Anderson, L. C.; Xu, M. T.; Mooney, C. E.; Rosynek, M. P.; Lunsford, J. H. *J. Am. Chem. Soc.* **1993**, *115* (14), 6322–6326.
- (55) Takanae, K.; Iglesia, E. *J. Phys. Chem. C* **2009**, *113* (23), 10131–10145.
- (56) Takanae, K.; Iglesia, E. *Angew. Chem. Int. Ed.* **2008**, *47* (40), 7689–7693.
- (57) Zhu, J. J.; van Ommen, J. G.; Lefferts, L. *Catal. Today* **2006**, *112* (1–4), 82–85.
- (58) Oliveira, M. C.; do Rego, A. M. B. *J. Alloys Compd.* **2006**, *425* (1–2), 64–68.
- (59) Naumkin, A. V.; Kraut-Vass, A.; Powell, C. J. *NIST X-ray Photoelectron Spectroscopy Database, Standard Reference Database 20, Version 3.5*; National Institute of Standards and Technology (NIST): Gaithersburg, MD; accessed in May 2012.
- (60) Branco, J. B.; Goncalves, A. P.; de Mato, A. P. *J. Alloys Compd.* **2008**, *465* (1–2), 361–366.
- (61) Panov, G. I.; Uriarte, A. K.; Rodkin, M. A.; Sobolev, V. I. *Catal. Today* **1998**, *41* (4), 365–385.